Review

A radical sense of direction: signalling and mechanism in cryptochrome magnetoreception

Charlotte A. Dodson[1], P.J. Hore[2], and Mark I. Wallace[1]

[1] Department of Chemistry, University of Oxford, Chemistry Research Laboratory, 12 Mansfield Road, Oxford OX1 3TA, UK
[2] Department of Chemistry, University of Oxford, Physical & Theoretical Chemistry Laboratory, South Parks Road, Oxford OX1 3QZ, UK

The remarkable phenomenon of magnetoreception in migratory birds and other organisms has fascinated biologists for decades. Much evidence has accumulated to suggest that birds sense the magnetic field of the Earth using photochemical transformations in cryptochrome flavoproteins. In the last 5 years this highly interdisciplinary field has seen advances in structural biology, biophysics, spin chemistry, and genetic studies in model organisms. We review these developments and consider how this chemical signal can be integrated into the cellular response.

Sensing magnetic fields using cryptochrome proteins

The ability to sense and respond to the magnetic field of the Earth has been reported in numerous organisms, and has been most widely studied in migratory birds [1–5]. Many of these responses appear to use tiny particles of magnetite (Fe_3O_4) formed within the cell [6–8], but others are thought to exploit a quantum effect in the cryptochrome family of proteins, which results in an iron-free chemical compass.

Like the magnetic compass needles used by humans for a thousand years, cryptochrome compasses should respond to the direction of the magnetic field of the Earth. However there are some notable differences: the avian compass is an inclination compass and is therefore sensitive to the angle between the magnetic field lines and the surface of the Earth (perpendicular at the magnetic poles, parallel at the magnetic equator). It requires low levels of light to function and is insensitive to absolute compass polarity (i.e., it can distinguish north/south from east/west, and pole-wards from equator-wards, but not north from south) [9]. Finally, oscillating radiofrequency fields at suitably tuned frequencies are expected to interfere with detection of the geomagnetic field [10–12].

Unusually perhaps, the question of cryptochrome magnetoreception has been approached from two very different disciplines. At one end of the spectrum, zoology, neurophysiology, and histology have been used to study bird behaviour [1,13,14], to identify the areas of the brain involved in magnetic orientation [2,15,16] and to provide clues about protein expression and localisation *in vivo* [17]. At the other end, spin chemists have computed and measured the behaviour of electron spins in model compounds and cryptochrome molecules *in vitro* [18,19], and made theoretical predictions about the ordering of receptor molecules required for a direction sensor [20–25].

Cryptochromes have been proposed as the receptor molecules in an iron-free compass for over a decade [26]. Their involvement is consistent with the observed zoology and neurophysiology, and the molecules themselves possess the properties required of them by theory. This area has been reviewed recently [2,19,27]. Nevertheless, the chain of evidence linking protein to phenotype is frustratingly circumstantial. Migratory birds are difficult, if not impossible, to breed in captivity and so studies with knockout mutants have not been performed. Likewise, there have been no studies in avian cell lines, and it will require ingenuity to devise a cellular assay for magneto-responses. These factors mean that the key molecular experiments normally used to tie down a phenotype to a causal chain of molecular components are missing.

In this Review we discuss recent advances in the spin chemistry and structural biology of cryptochrome proteins. The number of structures of cryptochrome-family proteins has almost doubled in the past 5 years, and the last few years have marked the publication of three important structures: the first full-length structure of an insect cryptochrome and the first two structures of a domain of a mammalian cryptochrome. There is now widespread evidence that cryptochrome proteins can undergo the chemistry necessary for a magnetic response, and the first direct measurements of magnetic fields resulting in an effect on chemical rate constants have been made. The gap between responses at the biophysical and whole-organism levels has begun to be filled by genetic complementation experiments on the fruitfly *Drosophila melanogaster* and we summarise these. Finally, we consider ways in which signal transduction might transform cryptochrome activation into a cellular response.

Classification of cryptochromes

The classification of cryptochromes has historically been based on their role in the circadian clock where, in mammals, they are repressors of CLOCK and BMAL [28–30]

Corresponding author: Dodson, C.A. (charlotte.dodson@chem.ox.ac.uk).
Keywords: magnetoreception; cryptochrome; photolyase; radical pair hypothesis.

0968-0004/$ – see front matter
 http://dx.doi.org/10.1016/j.tibs.2013.07.002

Glossary

Electron spin (singlet/triplet states): electrons have a quantum mechanical property known as spin, associated with which is a magnetic moment. A radical pair has two unpaired electrons, one on each radical, meaning that it can exist in a singlet state, with the two magnetic moments opposed (↑↓), or a triplet state, with the two magnetic moments aligned (↑↑). Like most biological molecules, the ground state of FAD in cryptochrome is the singlet state and it forms a singlet radical pair with Trp_C after light excitation. Reactions involving both electrons of the radical pair are spin-selective; that is, a singlet radical pair recombines to a singlet product, a triplet radical pair recombines (where thermodynamically feasible) to a triplet product. However reactions that do not involve both radicals (e.g., protonation/deprotonation reactions) proceed irrespective of the radical pair spin state.

Exchange interaction: the difference in energy between singlet and triplet states in the absence of other spin interactions is known as the exchange interaction, $J(r)$. It decays exponentially with the distance between the two electrons in the radical pair. If $J(r)$ is large compared to the hyperfine interactions, it blocks singlet–triplet interconversion and so prevents magnetic sensitivity. In cryptochromes, FAD and Trp_C are sufficiently far apart that $J(r)$ is small and interconversion between singlet and triplet states occurs. The exchange interaction is difficult to measure experimentally, although it has been extracted as a fitted parameter in the case of *Xenopus* CRY-DASH [69].

Hyperfine coupling: the magnetic interaction of an unpaired electron and a magnetic nucleus (e.g., ^{1}H or ^{14}N) is called the hyperfine coupling. Which nuclei in a radical have significant hyperfine couplings is determined principally by the extent of the molecular orbital that contains the unpaired electron. In both FAD and Trp radicals, the relevant orbital is delocalised over the isoalloxazine and indole rings, respectively, so that it is mainly the ring protons and nitrogens that have significant hyperfine interactions. In the FAD–Trp radical pair, the strength of the hyperfine interactions are such as to cause singlet–triplet interconversion on the nanosecond timescale. For an immobilised radical pair, the anisotropy of the hyperfine interactions can lead to the anisotropic magnetic response required of a magnetic compass sensor.

Magnetic field effect: a magnetic field effect is the change in a measured rate constant or the change in the population of a molecular species brought about by applying a magnetic field to a chemical reaction. According to the radical pair mechanism, the magnetic field of the Earth modifies the net rate of FAD–Trp_C recombination in cryptochromes, via its effect on singlet–triplet interconversion, leading to cryptochrome being used as a magnetic compass in certain organisms. Two crucial requirements for a magnetic field effect are that the non-equilibrium spin state of the radical pair (known as spin correlation) persists long enough for the rate of singlet/triplet interconversion to be altered by the geomagnetic field, and for the effect to be transferred to the reaction products.

timeless–GAL4/UAS–cryptochrome: Gal4 is a yeast transcription factor that binds to the UAS (upstream activation sequence) in the promoter of a second gene where it activates gene transcription. In the experiments in [79,86], a strain of flies was made with *GAL4* fused to the *timeless* gene and *cryptochrome* under the control of the UAS. Thus, in cells that normally express *timeless*, the TIMELESS–GAL4 construct will bind to the UAS and induce CRYPTOCHROME expression. This means that although the genetics of each cell in the fly is identical, CRYPTOCHROME expression is selectively induced in a subpopulation of tissues (those cells expressing TIMELESS).

Tryptophan triad: three highly conserved tryptophan residues (Trp_A, Trp_B, Trp_C; Trp_A closest to FAD, Trp_C on the protein surface) whose presence is key to the radical pair mechanism. The probability of through-space electron transfer decays approximately exponentially with increasing distance. A chain of three tryptophan residues spaced 4–6 Å apart shortens the distance of each transfer and thus vastly increases the probability of a radical pair forming between FAD and Trp_C compared with a single through-space transfer of 18 Å.

Zeeman interactions: the interaction of an external magnetic field (e.g., that of the Earth) with an electron spin is called a Zeeman interaction. For the Earth's magnetic field (~50 μT), these interactions decay on a timescale of ~700 ns. This means that in cryptochrome they are able to modify the rate of singlet–triplet interconversion of the FAD–Trp_C radical pair, giving rise to a magnetic field effect on the radical pair lifetime and on the yields of its chemical reaction products.

(Table 1). Those cryptochromes that were light sensitive and that acted as circadian photoreceptors in insects were designated Type I [31]. Type II cryptochromes were originally classified as cryptochromes with a light-independent (core component) role in the circadian clock and are widespread in mammals and in non-*Drosophila* insects [30]. Plant cryptochromes, although not part of this classification system, are also light sensitive and are responsible for the blue light growth response [32–34]. The circadian role of each cryptochrome in most species has not been determined, therefore, in practice, most cryptochrome classification is carried out by protein sequence alignment. Those cryptochromes proposed to be responsible for avian magnetoreception (cryptochromes in migratory birds such as the garden warbler, *Sylvia borin*, and the European robin, *Erithacus rubecula*) cluster with Type II cryptochromes in sequence alignments, despite the light dependence of their magnetoreceptive mechanism (see next section). CRY-DASH proteins form a fourth class of cryptochromes, which have a putative role in DNA repair and are found in many species [35–39].

Cryptochromes belong to the same family of proteins as a class of DNA repair proteins known as photolyases [40–42]. Structurally, both groups of proteins consist of a conserved photolyase homology region (PHR domain) that adopts a mostly helical fold and contains an FAD cofactor (Figure 1A–C). The PHR domain in photolyases usually contains a second cofactor [either methenyl-tetrahydrofolate (MTHF), or 8-hydroxy-deazaflavin (HDF)]. Photolyases consist solely of a PHR domain, but cryptochromes often possess additional N- and/or C-terminal extensions that vary widely between species and class of cryptochrome (Figure 1A). Both cryptochromes and photolyases maintain a striking pattern of conserved tryptophan residues in the PHR domain and a chain of three of these (termed Trp_A, Trp_B, and Trp_C, with Trp_A closest to the FAD and Trp_C nearest to the protein surface) appears to be key to magnetosensitivity (Figure 1D).

Cryptochrome photocycles and response to magnetic fields

The response of cryptochromes and photolyases to magnetic fields lies in the chemistry undergone by the bound FAD cofactor and the protein together, known as the radical pair mechanism [19,43,44] (Box 1). In this, a fully oxidised FAD molecule (FAD_{ox}) absorbs a photon (Figure 2C, reaction 1) and uses the energy to cycle through different oxidation states, forming a spin-correlated radical pair with the surface tryptophan residue Trp_C (the magnetically sensitive state) within picoseconds, before returning to the fully oxidised form within milliseconds [45–50] (Figure 2A,C). The effect of this cycle is that magnetic fields can alter the equilibrium population of different flavin oxidation states and thus any downstream signal that selects between them. The photocycles of many different cryptochromes, including that of CRY1 from the migratory garden warbler, have been studied *in vitro* [48,51–58] and the rate of return of the flavin to the ground state has been shown to be sensitive to magnetic fields for both *Escherichia coli* photolyase and CRY1 from *Arabidopsis thaliana* (*At*Cry1) [47,49]. Additional photocycles exist in the case of DNA repair by photolyases [40,59]: these involve transient radical pairs formed from the flavin and the substrate DNA, but there is no evidence that they are magnetically sensitive. An alternative radical pair has also been proposed between $FADH^{\bullet}$ and the superoxide radical $O_2^{\bullet-}$ which, in theory, would confer magnetic sensitivity on the dark reaction $FADH^{\bullet} \rightarrow FAD$ (Figure 2C, reaction 6) [18,60]. This mechanism currently remains a theoretical proposal for which there is only indirect experimental evidence [61].

Table 1. Classification of eukaryotic cryptochrome genes

	Organism	Gene name[a]	Uniprot
Type I[a]	*Drosophila melanogaster* (fruit-fly)	cry	O77059
	Anopheles gambiae (mosquito)	Cry1	Q7PYI7
	Danaus plexippus (monarch butterfly)	cry1	Q2TJN5
Plant	*Arabidopsis thaliana* (mouse-ear cress)	CRY1, 2	Q43125, Q96524
Type II[a]	*Sylvia borin* (garden warbler)[b]	CRY1, Cry1b	Q6ZZY0, Q0PGA8
	Erithacus rubecula (European robin)[b]	CRY1	Q5IZC5
	Gallus gallus (domestic chicken)[b]	CRY1, 2, 4	Q8QG61, Q8QG60, n/a
	Homo sapiens (human)	CRY1, 2	Q16526, Q49AN0
	Mus musculus (mouse)	Cry1, 2	P97784, Q9R194
	Xenopus laevis (African clawed frog)[b]	Cry1, 2a, 2b	Q90WY1, Q90WY0, Q90WX9
	Danio rerio (zebrafish)[b]	cry1a, 1b, 2a, 2b, 3	Q9I917, Q9I916, Q9I915, Q9I914, Q9I913
	Anopheles gambiae[b]	Cry2	Q0QW07
	Danaus plexippus	cry2	Q0QWP3
CRY–DASH	*Arabidopsis thaliana*	CRYD/CRY3	Q84KJ5
	Danio rerio	cry-dash	Q4KML2
	Xenopus laevis	cry-dash	Q75WS4
(6-4) photolyase	*Drosophila melanogaster*	phr6-4	Q0E8P0
	Arabidopsis thaliana	UVR3	O48652

[a]The cryptochrome class is distinct from the species-specific gene numbering (cry1, cry2, etc) and is generally referred to in roman numerals to reduce confusion.

[b]Assigned class based on sequence similarity.

Blue-light illumination of cryptochromes not only results in fast electron transfer from Trp_C to FAD_{ox} via the tryptophan triad, but also in protonation of the flavin (except in insect Type I cryptochromes; discussed later) and deprotonation of Trp_C [62]. Protonation of $FAD^{\bullet-}$ to form $FADH^{\bullet}$ occurs within microseconds in plant cryptochromes [47,48] and Fourier Transform Infra-Red spectroscopy (FTIR) suggests that the proton donor is an Asp, probably on the α16 helix (Figure 1B) [63,64]. This Asp is not conserved outside plants and the evidence suggests that in these cases a residue other than Asp is involved [51,65]. The physiological proton donor in non-plant, non-insect cryptochromes is not known, but protonation is likely to be slower than in plant cryptochromes; purely because the proton donor is not in the immediate vicinity of the isoalloxazine ring. FTIR experiments on *Xenopus* (6-4) photolyase, using low temperatures to trap short-lived species, confirmed that proton and electron transfer are two distinct events in the photocycle: at 200 K, FAD_{ox} was reduced to form $FAD^{\bullet-}$ (electron transfer) before going on to form $FADH^{\bullet}$ at 277 K (proton transfer) [51]. Driving this reaction in reverse in the photolyase from *Synechocystis* (i.e., oxidation of the semiquinone; in this case by molecular oxygen), shows the importance of several residues in the FAD binding pocket for the rate of proton transfer [66,67].

Deprotonation of $Trp_C^{\bullet+}$ occurs within microseconds for both *At*Cry1 and *E. coli* photolyase [47]. For *E. coli* the rate of this reaction depends on solvent glycerol concentration, and its mechanism is thus thought to be release of the proton to bulk solvent [45,47,68]. However, Trp_C deprotonation in the plant cryptochrome CPH1 from *Chlamydomonas reinhardtii* (which shares 46% sequence identity

Box 1. The radical pair mechanism in cryptochrome

Excitation of fully oxidised FAD by UV or blue light (<500 nm, see Figure 2B in main text) provides enough energy for the FAD to form an excited state (reaction 1, Figure 2C) and abstract an electron from the protein to form a spin-correlated radical pair (comprising the anionic flavin radical and the cationic radical of a nearby tryptophan residue, Trp_A). The Trp_A radical abstracts an electron from a second tryptophan (Trp_B), which in turn receives one from a third tryptophan on the protein surface (Trp_C), forming an electron transfer chain of three tryptophan residues (Figure 1D). The net result is that within picoseconds of light absorption [47–49,62,69], a spin-correlated radical pair is established comprising the cofactor flavin and a surface tryptophan residue 18 Å away (reaction 2, Figure 2C).

Normally a spin-correlated radical pair such as this would have too short a lifetime to be influenced by a magnetic field as weak as that of the Earth (50 μT). However, the decreasing redox potentials along the tryptophan chain [62] make the reverse flow of electrons from FAD to Trp_C slow enough for competition to exist between this pathway and others (7a competing with 3 and 4; Figure 2C).

Unpaired electrons (such as those in the flavin-tryptophan radical pair) possess a magnetic moment, which interacts with magnetic nuclei (e.g., ^{1}H, ^{14}N; hyperfine interactions) and with external magnetic fields (e.g., that of the Earth; Zeeman interactions). Additionally, the large separation of the two halves of the flavin–tryptophan radical pair (>15 Å) means that the singlet and triplet states are almost isoenergetic (the exchange and dipolar interactions are small). One consequence is that the flavin–Trp_C radical pair interconverts between singlet and triplet states (see Glossary) at frequencies determined by the hyperfine interactions and modified by the Zeeman interaction. In other words, the process of singlet–triplet interconversion (3) is affected by the presence or absence of external magnetic fields.

The radical pair can return to the ground state in many ways. Any return reaction involving both electrons in the radical pair (e.g., back electron transfer along the triad, 7a–c) will be spin-selective and only occur from the singlet state. The yield of such reactions will be magnetically sensitive because the population of the singlet radical pair state varies with the presence or absence of magnetic fields. Non-spin-selective oxidation/reduction of either radical [66,67] (6) will destroy the radical pair without giving rise to a magnetic field effect.

Crucially, reaction 7a must be slower than singlet-triplet mixing (3), but faster than the decay rate of the spin-correlation of the radical pair. The competing reactions of back electron transfer (7a) with (de)protonation (4,5) must also have similar rate constants to ensure that external magnetic fields have an effect on the chemistry of the system.

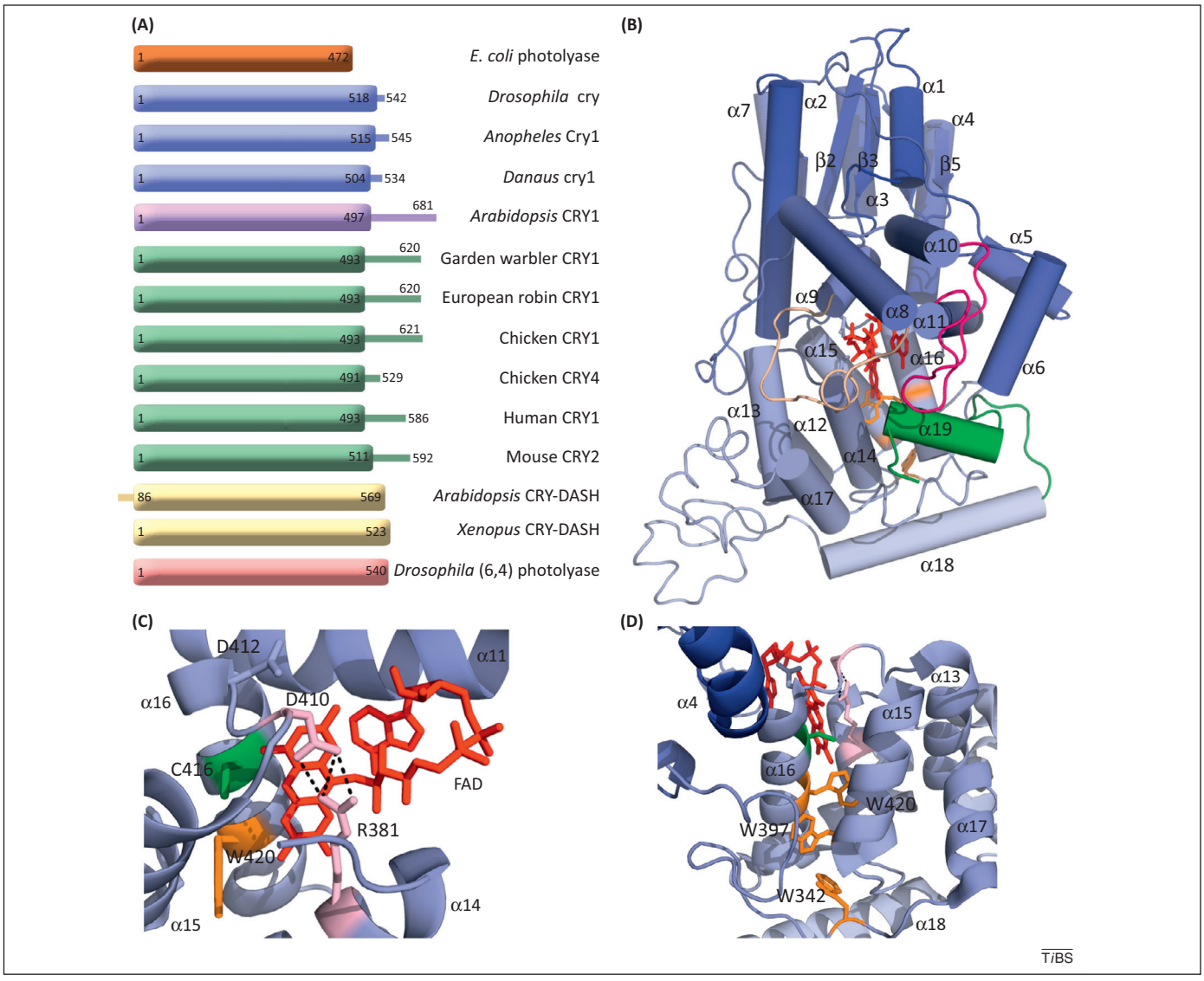

Figure 1. Cryptochrome domain and structural motifs. **(A)** Domain structures of selected cryptochromes and photolyases. Prokaryotic cyclobutane pyrimidine dimer (CPD) photolyase shown in brown, Type I cryptochromes in blue, plant-type cryptochrome in purple, Type II cryptochromes in green, CRY–DASH proteins in yellow, and (6,4) photolyase in red. The photolyase homology region (PHR) domain is shown as a rectangle, and N- and C-terminal extensions as lines. (B–D) structure of *Dm*Cry (PDB 4GU5). **(B)** Helices are labelled as in Table 2. PHR domain shown in blue to white, N to C terminus; C-terminal tail of 21 residues in green; α8/9 loop in beige; α10/11 loop ('protrusion motif' [75]) in bright pink, FAD in red. **(C)** FAD binding site showing DXD motif on α15/16 loop, highly conserved Arg–Asp salt bridge in light pink, photocycle modulating Cys on α16 (Asn in most cryptochromes, Asp in *At*Cry1) in green, and the beginning of the tryptophan triad (W420, Trp_A) in orange. FAD shown in red. **(D)** Tryptophan triad. Conserved Trp shown in orange stick representation in foreground: W420, Trp_A; W397, Trp_B; W342, Trp_C. Trp_C is found on the α11/12 loop shortly before the start of α12. Residues highlighted in (B) also visible towards rear. CPD, cyclobutane pyrimidine dimer; PHR, photolyase homology region.

with *At*Cry1) occurs within picoseconds and is thought to involve proton transfer from Trp_C to one of a number of histidine residues [45]. Interestingly, the magnetically sensitive state for both *At*Cry1 and *E. coli* photolyase is the radical pair formed initially (unprotonated $FAD^{\bullet-}$, protonated $Trp_C^{\bullet+}$). This is unlikely to result from some specific property of the protonated $Trp_C^{\bullet+}$ radical, and is more likely to arise because the spin correlation of the initial radical pair is too short lived for it to be propagated beyond this species [the lifetime measured in *Xenopus* CRY–DASH by electron paramagnetic resonance (EPR) spectroscopy is ~10 μs] [47,69].

Electron transfer (FAD reduction), FAD protonation, and Trp_C deprotonation are three distinct processes in cryptochrome-family proteins occurring in the first few microseconds after blue-light illumination. Each is modulated by different factors (e.g., different amino acid residues or different degrees of solvent exposure). Electron transfer is critical for magnetoreception and establishes the spin-correlated radical pair that is fundamental to the radical pair mechanism. The roles of FAD protonation and Trp_C deprotonation are less clear, but they appear to allow the effects of the magnetic field on the initial radical pair to be maintained in longer lived states of the protein. We speculate that these latter may be involved in signalling magnetically sensitive information to the cell.

Structure of cryptochromes

Of the 40 cryptochrome/photolyase structures in the PDB, 14 are of distinct protein sequences. The overall fold is maintained across the family, although there are differences in loop positioning and helical length between the

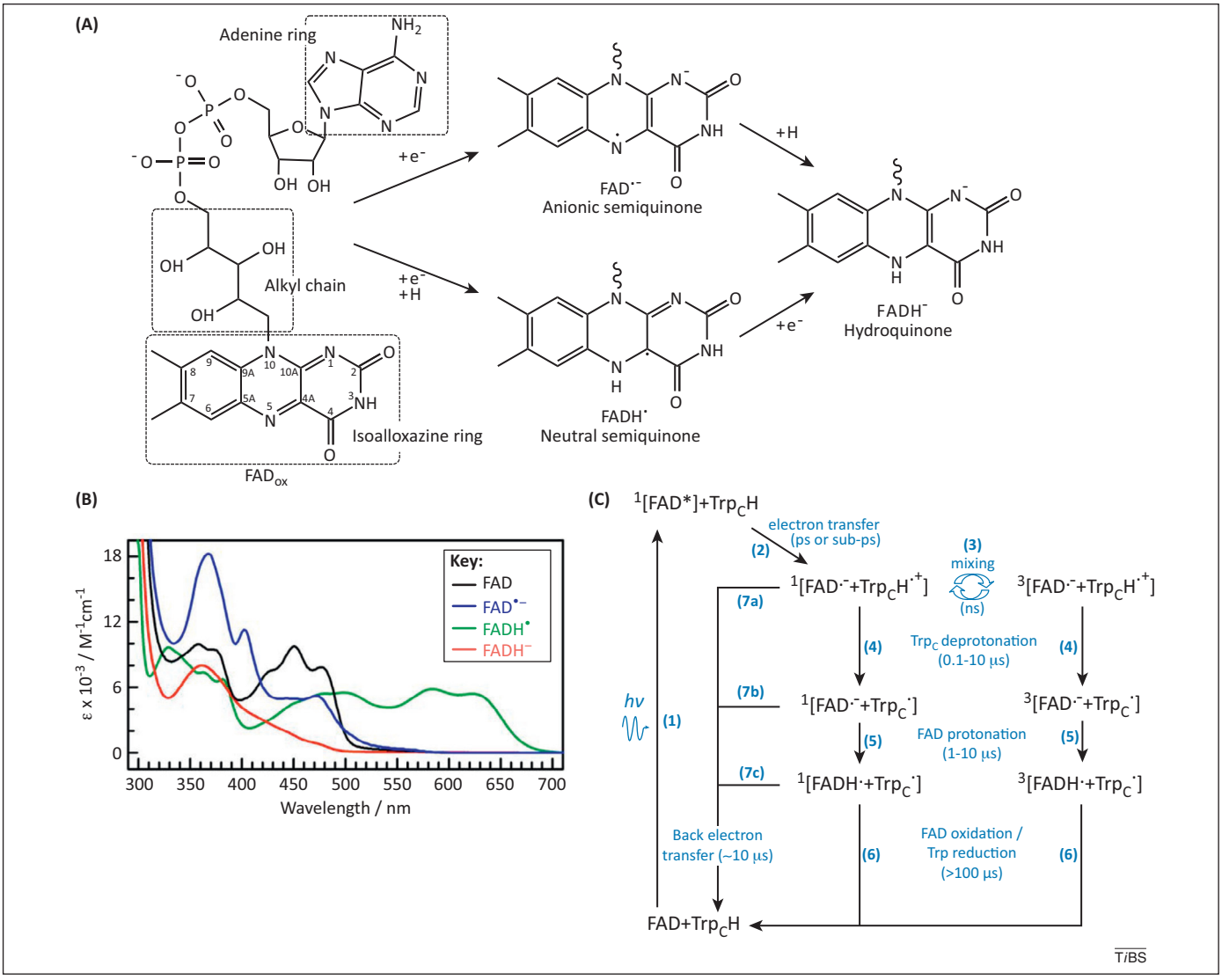

Figure 2. Physical properties of FAD. **(A)** Chemical structure of FAD and of the isoalloxazine ring in its biologically relevant oxidation states. **(B)** Absorption spectra of FAD oxidation states. Reproduced, with permission, from [100]. **(C)** Photocycle for cryptochrome magnetosensitivity. Approximate reaction timescales, based on experimental values, are given in brackets. Fully oxidised FAD is excited to ^{1}[FAD*] (1) [49,69,101], which decays within picoseconds to a singlet radical pair ^{1}[FAD$^{\bullet-}$ Trp$_C$H$^{\bullet+}$] (2). Singlet/triplet mixing of the radical pair (3) is modulated by magnetic fields and occurs on the nanosecond timescale. The spin-correlation of the radical pair has a lifetime of ~10 μs before spin-dephasing of singlet and triplet occurs (not shown) [69]. Protonation/deprotonation reactions are independent of electron spin and, in our scheme, deprotonation of Trp$_C$H$^{\bullet+}$ (4) precedes protonation of FAD$^{\bullet-}$ (5). We note that time-resolved measurements of these reactions are only available for a handful of cryptochromes/photolyases, some of which are likely to be exceptions to a general rule across the animal kingdom, and we expect the rate of (de)protonation to depend on the exact cryptochrome and experimental conditions [45,47–49,62]. There is no proton transfer to FAD$^{\bullet-}$ (5) in insect cryptochromes. Back electron transfer from the semiquinone to the Trp$_C$ radical to form the fully oxidised FAD (7) is spin-selective and only occurs from the singlet state. Other routes by which FAD radicals are oxidised and Trp radicals reduced (6) are spin-independent and will occur at the same rate irrespective of singlet/triplet populations.

different classes of molecule; presumably reflecting their different physiological roles (summarised in Table 2).

Most structures are of a single PHR domain from photolyases or CRY–DASH proteins, or of truncated cryptochrome constructs with no information on the conformation of the C-terminal tail. The only crystal structure of a full-length cryptochrome is that from *Drosophila melanogaster* [70–72] (Figure 1B). In this, the C-terminal extension is short (21 residues) and forms an additional helix (α19) that packs against the main body of the PHR domain in the cleft analogous to the active site for DNA repair in a photolyase/CRY–DASH. Intriguingly, this packing maintains a solvent channel, passing to one side of the helix, between the adenine ring of the FAD and the bulk solvent.

Recently, the structures of the first animal cryptochromes (mouse CRY1 and CRY2, *m*Cry1 and *m*Cry2) have been determined [72,73]. Intriguingly, neither cryptochrome purified with FAD bound, although *m*Cry2 could bind FAD *in vitro* with a K_d of 40 μM [73]. In both structures, the α8/9 ('phosphate binding') loop adopts a conformation similar to that in *Dm*Cry and the α10/11 loop is similar to that in *E. coli* photolyase; probably making this one of the most open FAD binding sites in a PHR domain and partially explaining the weak FAD binding.

Environment of the isoalloxazine ring

The orientation and oxidation state of the isoalloxazine ring of the flavin in the PHR domain is important for magnetoreception because it is this that undergoes the magnetically sensitive chemistry. In all structures, the FAD cofactor is held in a distinctive U-shaped conformation, with the alkyl chain packing against the adenine ring

Table 2. Cryptochrome/photolyase structures in the PDB

Classification				Organism	PDB	Other pdbs	Second co-factor	Trp triad	α16 flavin-interacting residue	Extensions beyond PHR domain	Loop variations	Refs
Eukaryotic	Cryptochrome	Type I	Insect	*Drosophila melanogaster* (fruit-fly)	4GU5 4JZY 4K03		No second cofactor found	W342 W397 W420	C416	Additional helix at CT (α19). Bound back into what would be photolyase active site.	Extended α5 helix. Helix α8 is extended compared to other structures giving a clear division between helix and α8/9 loop. α8/9 loop is displaced towards α2 at the C-terminal end, leaving a cavity open directly to the FAD. Extended α10/11 loop ('protrusion motif') is displaced towards helix α19 compared with (6-4) photolyases. Unlike the (6-4) photolyases, this sequence does not include a conserved Pro.	[70–72, 75,102]
		Plant	Plant	*Arabidopsis thaliana* (mouse-ear cress) CRY1	1U3C	1U3D		W324 W377 W400	D396	Truncated construct (PHR domain only) ending with α18.	Small turn of helix in β2/α2 loop displaced up towards α4 helix (and second cofactor binding site). Final turn of α5 unwound and α5/α6 loop adopting distinctive solvent-protruding conformation. Additional bent helix replaces loop between α7 and α8.	
		Type II	Animal	*Mus musculus* (mouse) CRY1	4K0R		No FAD or second cofactor found	W320 W374 W397	N393	Truncated construct (PHR domain only) ending with α18.	Centre of α8/9 loop similar to *Dm*Cry and displaced towards α2 leaving a cavity open to what would be the FAD binding site, but without the extended helix α8 found in *Dm*Cry. 4 residues in centre of loop not modelled in crystal structure and presumably disordered. Short α10/11 loop similar to that of *E. coli* photolyase but moved towards the C-terminal end of α6 (as for mouse CRY2).	[72]
		Type II	Animal	*M. musculus* (mouse) CRY2	4I6E	4I6G 4I6J	No FAD or second cofactor found	W338 W392 W415	N411	Truncated construct (PHR domain only). Unliganded structures end with α18, complex with SCF^{FBXL3} (4I6J) has 17 further residues.	First part of α8/9 loop (11 residues) not modelled in crystal structure and presumably disordered. Second half of α8/9 loop as for mouse CRY1. α10/11 loop similar to that of *E. coli* photolyase but moved towards the C-terminal end of α6 (as for mouse CRY1).	[73]
		CRY–DASH	Plant	*A. thaliana* (mouse-ear cress)	2IJG	2VTB	MTHF	W356 W409 W432	N428	NT helix (α0) rests against helix α8.	β2/α2 loop extended and oriented towards α15. Shorter than average sequence after α17, with some clusters of helical turns and no α18.	

	Photolyase	(6-4) photolyase	Insect	*D. melanogaster* (fruit fly)	3CVU	2WB2 2WQ6 2WQ7 3CVV 3CVW 3CVX 3CVY	8-HDF	W330 W384 W407	N403		β2/α2 loop extended and oriented towards α13. Extended α5 helix (as *Dm*Cry). α7 helix perpendicular to that in *Dm*Cry. α8/9 loop ('phosphate binding loop' in *Arabidopsis* (6-4) photolyase) contains a turn of 3_{10} helix which partially blocks DNA entry to the substrate binding cavity. Extended α10/11 loop forms a 'protrusion motif' that restricts entry to DNA binding cavity.	[75,102]
		(6-4) photolyase	Plant	*A. thaliana* (mouse-ear cress)	3FY4		8HDF	W329 W383 W406	N402	Additional helix at CT (α19). Not bound to protein core domain.	α8/9 loop ('phosphate binding loop') contains a turn of 3_{10} helix which partially blocks DNA entry to the substrate binding cavity. Extended α10/11 loop forms a 'protrusion motif' that restricts entry to DNA binding cavity.	[75,102]
		Class II CPD photolyase	Plant	*Oryza sativa* (rice)	2UMV		No second cofactor found	W378 W399 W406	N421 (α15)	Slightly truncated PHR domain. Helix α18 immediately follows α17 and is placed against α13.	Additional β0 strand (at N-terminus) and helix α7 placed closer to α18. Poss endogenous phosphorylation on S312 on helix α11.	[74,80]
Prokaryotic	Cryptochrome	CRY–DASH	Cyano-bacteria	*Synechocystis sp.* PCC 6301	1NP7			W320 W373 W396	N392		β2/α2 loop extended and oriented towards α15 (as in AtCry3/*Arabidopsis* CRY-DASH structure).	
	Photolyase	Class I CPD photolyase	Bacteria	*Escherichia coli*	1DNP		MTHF	W306 W359 W382	N378		Final turn of α5 unwound and α5/α6 loop adopting distinctive solvent-protruding conformation. Unique α10/11 loop which forms a turn of helix and does not approach DNA binding cavity.	
		Class I CPD photolyase	Bacteria	*Thermus thermophilus*	1IQR	1IQU 2J07 2J08 2J09		W275 W328 W351	N347		Shorter than average loop between α17 and α18, adopting less elaborate conformation.	
		Class I CPD photolyase	Cyano-bacteria	*Synechocystis sp.* PCC 6803	1QNF	1OWL 1OWM 1OWN 1OWO 1OWP 1TEZ	8HDF	W314 W367 W390	N386		Final turn of α5 unwound and α5/α6 loop adopting distinctive solvent-protruding conformation.	
		Class I CPD photolyase	Archaea	*Sulfolobus tokodaii* strain 7	2E0I		FAD as second cofactor	W274 W327 W350	N346			
		Class II CPD photolyase	Archaea	*Methanosarcina mazei* Go1	2XRY	2XRZ	No second cofactor detected	W360 W381 W388	N403 (α15)	Slightly truncated PHR domain. A truncated helix α18 follows the same conformation as in *Oryza*.	Additional β0 strand. α7/8 loop extends further towards α12 and helix α7 is placed closer to α18 (β0 and α7 as *Oryza*).	[77]

The helical numbering in this table is based loosely around the *Drosophila* cryptochrome structure, and intended to give a framework within which multiple cryptochrome structures can be compared (illustrated in Figure 1B). Helices are defined as (*Drosophila* numbering): α1 20-28; α2 53-75; α3 87-99; α4 111-129; α5 142-150; α6 157-169; α7 189-196; α8 226-248; α9 266-272; α10 276-289; α11 305-323; α12 346-355; α13 360-374; α14 377-389; α15 396-408; α16 412-426; α17 439-448; α18 497-517; α19 527-536.

and with the isoalloxazine ring angled slightly away from it. An Asp–Arg salt bridge is conserved across all cryptochromes and photolyases [74,75]. This involves the first Asp of the conserved DXD motif on the α15/16 loop and an Arg on α14 [Asp410–Arg381 in *Dm*Cry, Asp396–Arg367 in *Arabidopsis* (6,4) photolyase], such that the isoalloxazine ring of the FAD is inserted between this salt bridge and helix α16 (Figure 1C). Disruption of this bond (e.g., by the cry^b mutation in *Drosophila*) results in severe functional defects [75]. In many structures, the O4 oxygen of the isoalloxazine ring is held in place by hydrogen bonds to the backbone of the α15/16 loop (to the Asp residues of the DXD motif). Likewise, the N10 and N5 often form polar interactions with the α14 Arg from the salt bridge and a residue (normally an Asn) part-way up α16. The guanidinium moiety of the α14 Arg is positioned to stabilise the semiquinone radical at the C4a position [75].

The α16 Asn is important in tuning the redox potentials of the flavin and also in modulating proton transfer to the semiquinone [65,67,76]. This Asn is replaced by a Cys in insect Type I cryptochromes, and by an Asp in *At*Cry1, but it is conserved elsewhere. In Class II photolyases the functionally equivalent residue is found on α15 and additionally forms a putative H-bond with the O4 oxygen [74,77]. Asn, but not Asp, stabilises the $FADH^{\bullet}$ radical in *Dm*Cry, and Asp prevents further photoreduction to $FADH^{-}$ in *At*Cry1 [66,77,78]. The Cys residue in the insect cryptochromes appears to prevent protonation of the FAD. Consequently these molecules form the anionic semiquinone radical $FAD^{\bullet -}$, which is probably the signalling species in *Drosophila* [65,79]. Other residues in the isoalloxazine binding pocket have also been shown to modulate redox stability [66], but interestingly, the identity of the α16 Asn appears to be important in CLOCK/BMAL1 repression (a Type II cryptochrome function), suggesting that a functional redox-active FAD is required for this light-independent process [75]. Whether or not radical pairs have a role in this repression is not known.

Tryptophan triad

The tryptophan triad (Figure 1D) is conserved throughout all cryptochromes, CRY–DASH proteins, (6-4) photolyases, and Class I cyclobutane pyrimidine dimer (CPD) photolyases (residues concerned shown in Table 2). Fast electron transfer between these residues is required for formation of the radical pair and this is achieved by the indole rings of Trp_A and Trp_B being oriented so that the frontier orbitals overlap (i.e., an approximately parallel orientation of the rings). Both Trp_B and Trp_C form H-bonds that are conserved across eukaryotic Type I and II cryptochromes and (6-4) photolyases to the Met and Cys of a MXXNXXCXXIPW motif preceding Trp_C (the W of the motif) in the α11/12 loop [75]. These H-bonds prevent free rotation of the side chain about the C_α/C_β bond.

In Class II photolyases, the tryptophan triad is not conserved. Instead, a functionally equivalent triad appears to be present on the opposite face of the FAD with equivalent kinetics of electron transfer to the traditional triad (residues in Table 2) [74,77,80]. Interestingly, the Trp→Phe substitution at the Trp_A position of this triad resulted in complete loss of DNA repair activity, but 4.6% of activity remained after a similar substitution at Trp_B and 46% after substitution at Trp_C. This implies that the tryptophan triad in Class II photolyases is not the sole electron transfer pathway, and suggests that there is branching after Trp_B to another electron donor such as tyrosine [77].

Physiological magnetosensitive response in model organisms

Most of the literature on iron-free magnetosensitivity, consistent with cryptochromes and the radical pair mechanism, comes from studies on avian migration. However, for reasons already laid out, tying the whole-organism response down to a molecular phenotype will be much easier in a laboratory species that can be modified genetically. Although there is disagreement in the literature about the presence or absence of a magnetically sensitive physiological response in *Arabidopsis* [81,82], magnetic sensitivity has been addressed directly by preference experiments in *Drosophila*. This preference was slight and corresponded to ~57% of flies selecting one chamber over another in a binary choice T-maze assay, albeit in multiple replicates. The preference was wavelength dependent and was absent when wavelengths below 420 nm were blocked. Training with a sucrose reward reversed a naïve aversion to magnetic fields in wild type flies and, most notably, $cry^{-/-}$ and cry^b flies lacked either a naïve or trained response [83]. The period of the *Drosophila* circadian clock has been shown to be sensitive to magnetic fields in a cryptochrome-dependent manner [84], but the magnetic intensity sensing in the transgenic flies discussed here appears to be independent of the circadian response as both *timeless*- and *cycle*-deficient flies, whose circadian clocks are disrupted as a result of these mutations, retained magnetosensitivity in the T-tube selection assay [83]. The development of an assay to measure magnetic sensitivity in a model organism such as *Drosophila* is particularly exciting because it gives us the opportunity for extended genetic testing of the pathways and mechanisms involved.

In a series of experiments using *timeless–GAL4/UAS–cryptochrome*, both Type I [*Dm*Cry and cryptochrome 1 from the monarch butterfly (*Danaus plexippus, Dp*Cry1)] and Type II cryptochromes (*Dp*Cry2 and human *Hs*Cry2) have both been shown to rescue magnetosensitive choice in cry^b (D410N, functionless cryptochrome) flies [85,86]. In response to light, native *Dm*Cry is ubiquitylated and targeted to the proteasome [87,88]. Until recently it was thought that the substrate receptor in the E3 ligase complex responsible for targeting *Dm*Cry for ubiquitylation was JETLAG [87,89]. However, it now appears that although JETLAG binds *Dm*Cry in response to blue-light activation, JETLAG only functions as an E3 ligase for TIMELESS and the function of JETLAG binding to *Dm*Cry may be to entrain light-dependent degradation of TIMELESS [88,90]. Instead, the E3 ligase substrate receptor for *Dm*Cry is BRWD3 [88].

The degradation response to light is maintained in live *Drosophila* even when *Dm*Cry is replaced by *Hs*Cry1 (expressed using *timeless*-GAL4/UAS-*cryptochrome*) [79]. It is intriguing that downstream signalling is maintained

when *Dm*Cry is replaced by homologues from different species because the sequence of the C terminus, which has been shown to be responsible for several cryptochrome responses [87,91], diverges widely between these proteins. It suggests that BRWD3 and other signalling molecules bind to an epitope on the PHR domain, perhaps exposed by conformational change, rather than to an exposed patch on the C terminus itself. This prediction is supported by the structure of *m*Cry2 in complex with FBXL3, the substrate recognition component of the human E3 ligase complex SCF that targets *Hs*Cry1 and *Hs*Cry2 [73]. In this structure, the unstructured C terminus of FBXL3 penetrates to the FAD binding pocket of *m*Cry2, passing through the region that, in *Drosophila* cryptochrome, would be blocked by α19. Thus, we can envisage a model in which the C-terminal helix of *Dm*Cry protects the FAD binding site and hides the binding epitope for BRWD3. Under this model, blue light induces release of α19, allowing BRWD3 to bind, and resulting in proteasomal degradation of *Dm*Cry.

We would expect that a light-driven radical pair mechanism using cryptochromes would require an intact tryptophan triad. Surprisingly, substitution of Trp_C with phenylalanine in *Dp*Cry1 and *Dm*Cry in live flies does not appear to have any effect on magnetosensitivity, whereas a similar substitution in *Dp*Cry2 completely removes any magneto-response (although protein expression levels are stable) [86]. Substitution (Trp → Phe) of the tryptophan triad of protein overexpressed in insect cell culture does not affect the formation of the flavin radical at high light levels, but it does cause an impaired response at weaker illumination [79]. These data give us an apparent conflict between the radical pair hypothesis and some of the *in vivo* and cell culture experiments in which substitutions are made in the tryptophan chain. There is at present no good explanation of the different experimental results and, if this conflict is confirmed, either theoreticians will need to provide a new mechanism to describe magnetosensitivity in flies or experimentalists will need to find suitable partners to enable a spin-correlated radical pair to be formed in an intramolecular fashion within a cryptochrome–partner protein complex. One explanation may come from EPR experiments on *Xenopus* CRY–DASH mutants lacking an intact tryptophan chain. In these, a spin-correlated radical pair has been established between FAD and a tyrosine residue, presumed to be Tyr50 on the β2–α2 loop [92]. However, the length and positioning of this loop appears to be specific to CRY–DASH proteins and the generality of this result is unclear.

Transduction from a radical pair to downstream signalling

Within the framework of the radical pair mechanism, an applied magnetic field can only influence the recombination rate of the components of the radical pair. Although biophysically this is conceptually simple and has been measured *in vitro* (see above), it is less clear how this translates into a downstream cellular response. One elegant solution is that a magnetic field alters the equilibrium population of flavin oxidation states present under continuous illumination. If only one of these states is a signalling state then, as its population changes, so will its signalling output [19]. Such a solution would mean that signalling is never 'on' or 'off', but constantly giving a variable output reporting on local conditions as long as illumination is maintained.

What is the mechanistic implementation of a signalling state? FTIR data have implied that there are light-induced changes in the secondary structure of the PHR domains of CPH1 from *C. reinhardtii*, *Xenopus* (6-4) photolyase, and *Synechocystis* CRY–DASH, and changes in local hydrogen-bonding patterns upon forming $FADH^{\bullet}$ [51,64,65]. Such a small change could be expected to modulate the binding affinity between cryptochrome and a downstream signalling partner, or perhaps to modify the activity of the binding partner in a longer-lived interaction (Box 2). Photoreduction of $FADH^{\bullet}$ to $FADH^{-}$ has been studied structurally in crystals of photolyase from *Synechocystis*. In this experiment, illumination with red laser light or with X-rays neither disturbed the crystal lattice, nor resulted in

Box 2. Mechanism in downstream signal transduction

The radical pair mechanism explains how light energy can be transduced into chemical energy by cryptochrome proteins. However, these chemical changes must be integrated into the signalling pathways of the cell. The unusual suggestion that the charge-separated state in cryptochrome directly modulates the visual system is discussed in the main text. In this Box, we speculate on the more conventional ways in which chemical changes could be incorporated into cellular signalling. For all of these mechanisms, the signalling state of cryptochrome need not be the state with the longest lifetime.

Protein–protein interactions

In many biological processes, a signal-induced conformational change in one protein is propagated by a second partner binding in the presence of this change. If such a mechanism applies to magnetic signalling by cryptochromes (i.e., if a particular redox state promotes a protein–protein interaction) then the lifetime of the complex will ultimately determine the time-resolution of the magnetosensitivity of the cell.

Binding partner modulation

An alternative to the above model is that cryptochrome spends much of its time bound to a single partner (or a single complex of binding partners) and that the activity of the partner changes with the redox state of the cryptochrome. The interaction of the flavin with such a binding partner does not need to be direct or to involve proton/electron transfer, and could instead be modulated by changes in hydrogen bonding patterns or other subtle conformational changes. The partner could be an enzyme whose turnover or product binding is modulated, or perhaps an ion channel whose gating is altered. We emphasise that these examples are arbitrary and that there is no experimental evidence for either interaction. However, under this scenario the magnetic-field-dependent populations of the different cryptochrome oxidation states can be transduced into a longer-lived chemical signal (such as a protein modification or the concentration of a small molecule) that can be integrated with the conventional signalling of the cell.

Longer-lived conformational changes

As discussed in the main text, there is evidence for longer-lived conformational changes involving the C terminus for a number of cryptochromes following exposure to light. These often lead to protein ubiquitylation and degradation, and are perhaps the most concrete evidence of a cryptochrome response. Transduction of magnetically sensitive information by the degradation response or by these conformational changes is beyond the scope of this article.

any structural change beyond sub-Ångström movements of Asp380 (the first Asp of DXD motif) and Asn386 (on α16) [93]. Thus, this photoreduction reaction can occur without significant changes in secondary structure.

Limited proteolysis and immunoprecipitation have indicated light-induced changes in the conformation of the C-terminal extensions of *At*Cry1, *Dm*Cry, and chicken CRY4 from retinal cells. No such changes were detected in zebrafish cry4, which shares 62% sequence identity with the chicken cryptochrome [72,87,94,95]. Transient grating spectroscopy detected a change in the diffusion coefficient of *At*Cry1 (i.e., a conformational change) following blue-light excitation; the authors mapped this to the C terminus and showed that it required an intact tryptophan chain [96]. *Dm*Cry is stabilised in cell culture by the dark, and also by the presence of the circadian regulator TIMELESS [70]. *Dm*Cry lacking the C terminus is constitutively active and interacts with JETLAG in the absence of light [87], whereas interactions between the C terminus of *At*Cry1 and its binding partners enable light-regulated seedling growth [91]. Interestingly, it is not only C-terminal rearrangements that can lead to constitutive activity because the G380R substitution in *At*Cry1 (G380 is on α15, 3 Å from Trp_A and the substitution is likely to significantly disturb local structure) leads to a constitutive light response [97].

There is limited information on the timescales of C-terminal rearrangement. Western blots of trypsin hypersensitivity indicate that the light-induced state of *Dm*Cry has a half-life of 15 min in the dark in flies, and also that the light-induced conformational change is maintained independently of redox status [87]. The rate constant for rearrangement of *At*Cry1 from transient grating measurements is 2.5 s^{-1} ($\tau = 0.4$ s), and again, light-induced changes are retained even after reoxidation of the FAD [96]. Both timescales are considerably longer than the timescale of a cryptochrome photocycle and effectively decouple the structural and redox changes in cryptochrome. A long timescale is ideal for signalling the presence of light after a period of darkness, but achieving a magnetically sensitive response in this manner is much more complicated.

In a completely complementary approach, an entirely physical model of cryptochrome signal transduction has also been proposed [98]. Much evidence suggests that the avian magnetoreceptor is located in the retina [2,99], and this model relies on the local electrostatic field of a long-lived charge-separated state in cryptochrome modulating the *cis/trans* isomerisation of retinal in rhodopsin. Magnetoreception would thus have a direct effect on avian vision. For the electric field to be large enough for this to occur, the cryptochrome and rhodopsin molecules would need to be in close contact. Consistent with this, avian CRY1a has been found localised to the UV/violet cone cells of the retina of the European robin and the domestic chicken, in close proximity to the opsins [17]. However, there is no precedent for electric field effects on rhodopsin and this is at present a theoretical suggestion that requires direct experimental testing.

Concluding remarks

Cryptochromes are still the most likely candidate molecules to be used by migratory birds and other animals to sense and respond to the direction of the Earth's magnetic field. The past 2 years have seen PDB depositions of the first two structures of an animal cryptochrome and the structure of *Dm*Cry, the first full-length cryptochrome structure. Radical pairs have been measured in several cryptochromes and magnetic field effects have been detected in both *At*Cry1 and *E. coli* photolyase. *Drosophila* is being established as a model organism for magnetic behavioural assays and the first genetic experiments have now been conducted.

Here, we have comprehensively reviewed the information available on the structural biology of cryptochromes and the related photolyases, outlined the radical pair mechanism, and presented the most recent experimental findings from spin chemistry. The experiments *in vitro* and modelling are clear, but their relevance *in vivo* needs to be determined: for example, does endogenous cryptochrome *in vivo* follow the same photocycle as that *in vitro*? Which of the four avian cryptochromes is responsible for magnetoreception? What is the physiological redox state of endogenous cryptochrome in live cells and is this affected by the cellular redox environment? We have also summarised the *Drosophila* behavioural experiments and begun to address the question of signal transduction from cryptochrome to cellular response. This last area is poorly understood, and teasing out the different interactions and their magnetic sensitivities in a robust model will be one of the next big challenges in this field.

Acknowledgements

We would like to thank Till Biskup and Christiane Timmel for helpful discussions. Our research is funded by DARPA (grant no: QuBE N66001-10-1-4061) and the EMF Biological Research Trust.

References

1 Wiltschko, R. *et al.* (2010) Directional orientation of birds by the magnetic field under different light conditions. *J. R. Soc. Interface* 7 (Suppl. 2), S163–S177
2 Mouritsen, H. and Hore, P.J. (2012) The magnetic retina: light-dependent and trigeminal magnetoreception in migratory birds. *Curr. Opin. Neurobiol.* 22, 343–352
3 Ritz, T. (2011) Quantum effects in biology: bird navigation. *Proc. Chem.* 3, 262–275
4 Lohmann, K.J. (2010) Q&A: animal behaviour: magnetic-field perception. *Nature* 464, 1140–1142
5 Wiltschko, W. and Wiltschko, R. (2005) Magnetic orientation and magnetoreception in birds and other animals. *J. Comp. Physiol. A: Neuroethol. Sens. Neural Behav. Physiol.* 191, 675–693
6 Winklhofer, M. and Kirschvink, J.L. (2010) A quantitative assessment of torque-transducer models for magnetoreception. *J. R. Soc. Interface* 7 (Suppl. 2), S273–S289
7 Kirschvink, J.L. and Gould, J.L. (1981) Biogenic magnetite as a basis for magnetic field detection in animals. *Biosystems* 13, 181–201
8 Kirschvink, J.L. *et al.* (2001) Magnetite-based magnetoreception. *Curr. Opin. Neurobiol.* 11, 462–467
9 Wiltschko, R. and Wiltschko, W. (2006) Magnetoreception. *Bioessays* 28, 157–168
10 Henbest, K.B. *et al.* (2004) Radio frequency magnetic field effects on a radical recombination reaction: a diagnostic test for the radical pair mechanism. *J. Am. Chem. Soc.* 126, 8102–8103
11 Ritz, T. *et al.* (2004) Resonance effects indicate a radical-pair mechanism for avian magnetic compass. *Nature* 429, 177–180
12 Thalau, P. *et al.* (2005) Magnetic compass orientation of migratory birds in the presence of a 1.315 MHz oscillating field. *Naturwissenschaften* 92, 86–90

13 Phillips, J.B. *et al.* (2010) A behavioral perspective on the biophysics of the light-dependent magnetic compass: a link between directional and spatial perception? *J. Exp. Biol.* 213, 3247–3255
14 Wiltschko, R. and Wiltschko, W. (2007) Magnetoreception in birds: two receptors for two different tasks. *J. Ornithol.* 148, S61–S76
15 Nemec, P. *et al.* (2001) Neuroanatomy of magnetoreception: the superior colliculus involved in magnetic orientation in a mammal. *Science* 294, 366–368
16 Zapka, M. *et al.* (2009) Visual but not trigeminal mediation of magnetic compass information in a migratory bird. *Nature* 461, 1274–1277
17 Niessner, C. *et al.* (2011) Avian ultraviolet/violet cones identified as probable magnetoreceptors. *PLoS ONE* 6, e20091
18 Maeda, K. *et al.* (2008) Chemical compass model of avian magnetoreception. *Nature* 453, 387–390
19 Rodgers, C.T. and Hore, P.J. (2009) Chemical magnetoreception in birds: the radical pair mechanism. *Proc. Natl. Acad. Sci. U.S.A.* 106, 353–360
20 Cintolesi, F. *et al.* (2003) Anisotropic recombination of an immobilized photoinduced radical pair in a 50-mu T magnetic field: a model avian photomagnetoreceptor. *Chem. Phys.* 294, 385–399
21 Hill, E. and Ritz, T. (2010) Can disordered radical pair systems provide a basis for a magnetic compass in animals? *J. R. Soc. Interface* 7 (Suppl. 2), S265–S271
22 Lau, J.C. *et al.* (2012) Compass magnetoreception in birds arising from photo-induced radical pairs in rotationally disordered cryptochromes. *J. R. Soc. Interface* 9, 3329–3337
23 Lau, J.C. *et al.* (2010) Effects of disorder and motion in a radical pair magnetoreceptor. *J. R. Soc. Interface* 7 (Suppl. 2), S257–S264
24 Solov'yov, I.A. *et al.* (2007) Magnetic field effects in *Arabidopsis thaliana* cryptochrome-1. *Biophys. J.* 92, 2711–2726
25 Solov'yov, I.A. *et al.* (2010) Acuity of a cryptochrome and vision-based magnetoreception system in birds. *Biophys. J.* 99, 40–49
26 Ritz, T. *et al.* (2000) A model for photoreceptor-based magnetoreception in birds. *Biophys. J.* 78, 707–718
27 Liedvogel, M. and Mouritsen, H. (2010) Cryptochromes – a potential magnetoreceptor: what do we know and what do we want to know? *J. R. Soc. Interface* 7 (Suppl. 2), S147–S162
28 Yuan, Q. *et al.* (2007) Insect cryptochromes: gene duplication and loss define diverse ways to construct insect circadian clocks. *Mol. Biol. Evol.* 24, 948–955
29 Zhu, H. *et al.* (2005) The two CRYs of the butterfly. *Curr. Biol.* 15, R953–R954
30 Zhan, S. *et al.* (2011) The monarch butterfly genome yields insights into long-distance migration. *Cell* 147, 1171–1185
31 Hardin, P.E. (2011) Molecular genetic analysis of circadian timekeeping in *Drosophila*. *Adv. Genet.* 74, 141–173
32 Ahmad, M. and Cashmore, A.R. (1993) HY4 gene of *A. thaliana* encodes a protein with characteristics of a blue-light photoreceptor. *Nature* 366, 162–166
33 Chaves, I. *et al.* (2011) The cryptochromes: blue light photoreceptors in plants and animals. *Annu. Rev. Plant Biol.* 62, 335–364
34 Kami, C. *et al.* (2010) Light-regulated plant growth and development. *Curr. Top. Dev. Biol.* 91, 29–66
35 Brudler, R. *et al.* (2003) Identification of a new cryptochrome class. Structure, function, and evolution. *Mol. Cell* 11, 59–67
36 Froehlich, A.C. *et al.* (2010) Genetic and molecular characterization of a cryptochrome from the filamentous fungus *Neurospora crassa*. *Eukaryot. Cell* 9, 738–750
37 Kizilel, R. *et al.* (2012) Investigation of real-time photorepair activity on DNA via surface plasmon resonance. *PLoS ONE* 7, e44392
38 Pokorny, R. *et al.* (2008) Recognition and repair of UV lesions in loop structures of duplex DNA by DASH-type cryptochrome. *Proc. Natl. Acad. Sci. U.S.A.* 105, 21023–21027
39 Selby, C.P. and Sancar, A. (2006) A cryptochrome/photolyase class of enzymes with single-stranded DNA-specific photolyase activity. *Proc. Natl. Acad. Sci. U.S.A.* 103, 17696–17700
40 Brettel, K. and Byrdin, M. (2010) Reaction mechanisms of DNA photolyase. *Curr. Opin. Struct. Biol.* 20, 693–701
41 Muller, M. and Carell, T. (2009) Structural biology of DNA photolyases and cryptochromes. *Curr. Opin. Struct. Biol.* 19, 277–285
42 Sancar, A. (2003) Structure and function of DNA photolyase and cryptochrome blue-light photoreceptors. *Chem. Rev.* 103, 2203–2237
43 Rodgers, C.T. (2009) Magnetic field effects in chemical systems. *Pure Appl. Chem.* 81, 19–43
44 Steiner, U.E. and Ulrich, T. (1989) Magnetic-field effects in chemical-kinetics and related phenomena. *Chem. Rev.* 89, 51–147
45 Immeln, D. *et al.* (2012) Primary events in the blue light sensor plant cryptochrome: intraprotein electron and proton transfer revealed by femtosecond spectroscopy. *J. Am. Chem. Soc.* 134, 12536–12546
46 Lukacs, A. *et al.* (2008) Electron hopping through the 15 A triple tryptophan molecular wire in DNA photolyase occurs within 30 ps. *J. Am. Chem. Soc.* 130, 14394–14395
47 Maeda, K. *et al.* (2012) Magnetically sensitive light-induced reactions in cryptochrome are consistent with its proposed role as a magnetoreceptor. *Proc. Natl. Acad. Sci. U.S.A.* 109, 4774–4779
48 Langenbacher, T. *et al.* (2009) Microsecond light-induced proton transfer to flavin in the blue light sensor plant cryptochrome. *J. Am. Chem. Soc.* 131, 14274–14280
49 Henbest, K.B. *et al.* (2008) Magnetic-field effect on the photoactivation reaction of *Escherichia coli* DNA photolyase. *Proc. Natl. Acad. Sci. U.S.A.* 105, 14395–14399
50 Byrdin, M. *et al.* (2010) Quantum yield measurements of short-lived photoactivation intermediates in DNA photolyase: toward a detailed understanding of the triple tryptophan electron transfer chain. *J. Phys. Chem. A* 114, 3207–3214
51 Yamada, D. *et al.* (2012) Fourier-transform infrared study of the photoactivation process of *Xenopus* (6-4) photolyase. *Biochemistry* 51, 5774–5783
52 Song, S.H. *et al.* (2007) Formation and function of flavin anion radical in cryptochrome 1 blue-light photoreceptor of monarch butterfly. *J. Biol. Chem.* 282, 17608–17612
53 Kao, Y.T. *et al.* (2008) Ultrafast dynamics and anionic active states of the flavin cofactor in cryptochrome and photolyase. *J. Am. Chem. Soc.* 130, 7695–7701
54 Brazard, J. *et al.* (2010) Spectro-temporal characterization of the photoactivation mechanism of two new oxidized cryptochrome/photolyase photoreceptors. *J. Am. Chem. Soc.* 132, 4935–4945
55 Zirak, P. *et al.* (2009) Photocycle dynamics of the E149A mutant of cryptochrome 3 from *Arabidopsis thaliana*. *J. Photochem. Photobiol. B* 97, 94–108
56 Berndt, A. *et al.* (2007) A novel photoreaction mechanism for the circadian blue light photoreceptor *Drosophila* cryptochrome. *J. Biol. Chem.* 282, 13011–13021
57 Liedvogel, M. *et al.* (2007) Chemical magnetoreception: bird cryptochrome 1a is excited by blue light and forms long-lived radical-pairs. *PLoS ONE* 2, e1106
58 Giovani, B. *et al.* (2003) Light-induced electron transfer in a cryptochrome blue-light photoreceptor. *Nat. Struct. Biol.* 10, 489–490
59 Weber, S. (2005) Light-driven enzymatic catalysis of DNA repair: a review of recent biophysical studies on photolyase. *Biochim. Biophys. Acta* 1707, 1–23
60 Ritz, T. *et al.* (2009) Magnetic compass of birds is based on a molecule with optimal directional sensitivity. *Biophys. J.* 96, 3451–3457
61 Hogben, H.J. *et al.* (2009) Possible involvement of superoxide and dioxygen with cryptochrome in avian magnetoreception: Origin of Zeeman resonances observed by in vivo EPR spectroscopy. *Chem. Phys. Lett.* 480, 118–122
62 Aubert, C. *et al.* (2000) Intraprotein radical transfer during photoactivation of DNA photolyase. *Nature* 405, 586–590
63 Kottke, T. *et al.* (2006) Blue-light-induced changes in *Arabidopsis* cryptochrome 1 probed by FTIR difference spectroscopy. *Biochemistry* 45, 2472–2479
64 Immeln, D. *et al.* (2010) Photoreaction of plant and DASH cryptochromes probed by infrared spectroscopy: the neutral radical state of flavoproteins. *J. Phys. Chem. B* 114, 17155–17161
65 Iwata, T. *et al.* (2010) Key dynamics of conserved asparagine in a cryptochrome/photolyase family protein by fourier transform infrared spectroscopy. *Biochemistry* 49, 8882–8891
66 Damiani, M.J. *et al.* (2009) Kinetic stability of the flavin semiquinone in photolyase and cryptochrome-DASH. *Biochemistry* 48, 11399–11411
67 Damiani, M.J. *et al.* (2011) Impact of the N5-proximal Asn on the thermodynamic and kinetic stability of the semiquinone radical in photolyase. *J. Biol. Chem.* 286, 4382–4391

68 Byrdin, M. *et al.* (2004) Intraprotein electron transfer and proton dynamics during photoactivation of DNA photolyase from *E. coli*: review and new insights from an "inverse" deuterium isotope effect. *Biochim. Biophys. Acta* 1655, 64–70
69 Biskup, T. *et al.* (2009) Direct observation of a photoinduced radical pair in a cryptochrome blue-light photoreceptor. *Angew. Chem. Int. Ed. Engl.* 48, 404–407
70 Zoltowski, B.D. *et al.* (2011) Structure of full-length *Drosophila* cryptochrome. *Nature* 480, 396–399
71 Levy, C. *et al.* (2013) Updated structure of *Drosophila* cryptochrome. *Nature* 495, E3–E4
72 Czarna, A. *et al.* (2013) Structures of *Drosophila* cryptochrome and mouse cryptochrome1 provide insight into circadian function. *Cell* 153, 1394–1405
73 Xing, W. *et al.* (2013) SCFFBXL3 ubiquitin ligase targets cryptochromes at their cofactor pocket. *Nature* 496, 64–68
74 Hitomi, K. *et al.* (2012) Eukaryotic class II cyclobutane pyrimidine dimer photolyase structure reveals basis for improved ultraviolet tolerance in plants. *J. Biol. Chem.* 287, 12060–12069
75 Hitomi, K. *et al.* (2009) Functional motifs in the (6-4) photolyase crystal structure make a comparative framework for DNA repair photolyases and clock cryptochromes. *Proc. Natl. Acad. Sci. U.S.A.* 106, 6962–6967
76 Balland, V. *et al.* (2009) What makes the difference between a cryptochrome and DNA photolyase? A spectroelectrochemical comparison of the flavin redox transitions. *J. Am. Chem. Soc.* 131, 426–427
77 Kiontke, S. *et al.* (2011) Crystal structures of an archaeal class II DNA photolyase and its complex with UV-damaged duplex DNA. *EMBO J.* 30, 4437–4449
78 Burney, S. *et al.* (2012) Single amino acid substitution reveals latent photolyase activity in *Arabidopsis* cry1. *Angew. Chem. Int. Ed. Engl.* 51, 9356–9360
79 Hoang, N. *et al.* (2008) Human and *Drosophila* cryptochromes are light activated by flavin photoreduction in living cells. *PLoS Biol.* 6, e160
80 Okafuji, A. *et al.* (2010) Light-induced activation of class II cyclobutane pyrimidine dimer photolyases. *DNA Repair (Amst.)* 9, 495–505
81 Ahmad, M. *et al.* (2007) Magnetic intensity affects cryptochrome-dependent responses in *Arabidopsis thaliana*. *Planta* 225, 615–624
82 Harris, S.R. *et al.* (2009) Effect of magnetic fields on cryptochrome-dependent responses in *Arabidopsis thaliana*. *J. R. Soc. Interface* 6, 1193–1205
83 Gegear, R.J. *et al.* (2008) Cryptochrome mediates light-dependent magnetosensitivity in *Drosophila*. *Nature* 454, 1014–1018
84 Yoshii, T. *et al.* (2009) Cryptochrome mediates light-dependent magnetosensitivity of *Drosophila*'s circadian clock. *PLoS Biol.* 7, e1000086
85 Foley, L.E. *et al.* (2011) Human cryptochrome exhibits light-dependent magnetosensitivity. *Nat. Commun.* 2, 356
86 Gegear, R.J. *et al.* (2010) Animal cryptochromes mediate magnetoreception by an unconventional photochemical mechanism. *Nature* 463, 804–807
87 Ozturk, N. *et al.* (2011) Reaction mechanism of *Drosophila* cryptochrome. *Proc. Natl. Acad. Sci. U.S.A.* 108, 516–521
88 Ozturk, N. *et al.* (2013) Ramshackle (Brwd3) promotes light-induced ubiquitylation of *Drosophila* cryptochrome by DDB1-CUL4-ROC1 E3 ligase complex. *Proc. Natl. Acad. Sci. U.S.A.* 110, 4980–4985
89 Peschel, N. *et al.* (2009) Light-dependent interactions between the *Drosophila* circadian clock factors cryptochrome, jetlag, and timeless. *Curr. Biol.* 19, 241–247
90 Koh, K. *et al.* (2006) JETLAG resets the *Drosophila* circadian clock by promoting light-induced degradation of TIMELESS. *Science* 312, 1809–1812
91 Fankhauser, C. and Ulm, R. (2011) Light-regulated interactions with SPA proteins underlie cryptochrome-mediated gene expression. *Genes Dev.* 25, 1004–1009
92 Biskup, T. *et al.* (2013) Variable electron-transfer pathways in an amphibian cryptochrome: tryptophan versus tyrosine-based radical pairs. *J. Biol. Chem.* 288, 9249–9260
93 Kort, R. *et al.* (2004) DNA apophotolyase from *Anacystis nidulans*: 1.8 A structure, 8-HDF reconstitution and X-ray-induced FAD reduction. *Acta Crystallogr. D: Biol. Crystallogr.* 60, 1205–1213
94 Partch, C.L. *et al.* (2005) Role of structural plasticity in signal transduction by the cryptochrome blue-light photoreceptor. *Biochemistry* 44, 3795–3805
95 Watari, R. *et al.* (2012) Light-dependent structural change of chicken retinal cryptochrome4. *J. Biol. Chem.* 287, 42634–42641
96 Kondoh, M. *et al.* (2011) Light-induced conformational changes in full-length *Arabidopsis thaliana* cryptochrome. *J. Mol. Biol.* 413, 128–137
97 Gu, N.N. *et al.* (2012) Substitution of a conserved glycine in the PHR domain of *Arabidopsis* cryptochrome 1 confers a constitutive light response. *Mol. Plant* 5, 85–97
98 Stoneham, A.M. *et al.* (2012) A new type of radical-pair-based model for magnetoreception. *Biophys. J.* 102, 961–968
99 Moller, A. *et al.* (2004) Retinal cryptochrome in a migratory passerine bird: a possible transducer for the avian magnetic compass. *Naturwissenschaften* 91, 585–588
100 Liu, B. *et al.* (2010) Searching for a photocycle of the cryptochrome photoreceptors. *Curr. Opin. Plant Biol.* 13, 578–586
101 Weber, S. *et al.* (2010) Origin of light-induced spin-correlated radical pairs in cryptochrome. *J. Phys. Chem. B* 114, 14745–14754
102 Selby, C.P. and Sancar, A. (2012) The second chromophore in *Drosophila* photolyase/cryptochrome family photoreceptors. *Biochemistry* 51, 167–171